Original scientific paper

EFFECTS OF MONITORING SIGNAL HYSTERESIS ON SPEED REGULATION FOR THE AERO-DERIVATIVE GAS TURBINE

Zhibin Zhao[1, 2], Wenjie Zhou[1], Peijun Liu[2], Zhirui Liu[2]

[1]School of Energy and Power Engineering, Jiangsu University, Zhenjiang, China
[2]Institute of Engineering Thermophysics, Chinese Academy of Sciences, Beijing, China

Abstract*: Sensor aging and sensor failure are the common phenomena due to the high temperature and pressure environment for gas turbines, which can lead to hysteresis of monitoring signals. In this paper, a kind of aero-derivative gas turbine is taken as the research object. The hysteresis effects of single monitoring signal and coupling of multiple monitoring signals on speed control are mainly studied, and the analysis is carried out from the perspective of adjustment time, overshoot, fuel quantity and fuel quantity regulation output. The analysis results show that the pressure signal hysteresis will lead to speed suspension. The speed signal hysteresis will change the speed regulation into a multi-step mode. When the monitoring signal hysteresis is coupled, the effect of pressure signal hysteresis is greater than that of speed signal hysteresis. The results of this paper can provide a reference for the optimal design of speed control of aero-derivative gas turbine.*

Key Words*: Aero-derivative gas turbine, Pressure signal hysteresis, Speed signal hysteresis, Hysteresis coupling, Multi-step mode*

1. INTRODUCTION

As the core equipment of the power generation system, the aero-derivative gas turbine is an indispensable energy-converting device [1]. The aero-derivative gas turbine is developed based on the mature air engine technology. It retains most of the structure of the air engine and only adds the power turbine at the end of the gas generator. Therefore, the aero-derivative gas turbine inherits most of the advantages of the air engine and has the advantages of large power per unit volume, light weight, fast starting, good acceleration and high reliability [2, 3], it has become an important energy conversion equipment and power plant in the industrial field. At present, the aero-derivative gas turbine has been

widely used in various fields [4, 5], such as distributed energy, pipeline compression, marine power, mobile power station, power plant and offshore platform.

Gas turbine control technology is one of the core technologies in gas turbine, and it is also an important guarantee for the economy of gas turbine units. From the perspective of development, gas turbine control system has experienced the stages from the mechanical hydraulic control, analog electronic control to digital electronic control [6]. With the application of low emission combustion control technology, adaptive control technology, remote network control technology, intelligent sensors and actuators in the control system [7-10], the gas turbine control system is gradually developing towards integrated control, network control and active control.

PID algorithm is the earliest practical control algorithm, it is still the most commonly used control law in the control system. With the development of control theory, fuzzy control, particle swarm optimization algorithm, genetic algorithm and neural network model combined with PID algorithm are widely used in the field of control engineering to adapt to more complex controlled objects [11-14]. Less attention has been paid to the problems that the PID algorithm iteration results are biased due to the hysteresis of the monitoring signal, which causes the control system to send wrong instructions to the controlled object, and then leads to the slow adjustment of the control system and the deterioration of robustness.

The hysteresis of monitoring signal mainly comes from two aspects: on the one hand, it is caused by sensor failure, on the other hand, it comes from the control system. Gas turbines usually operate under complex conditions, such as high temperature, high pressure, etc. For monitoring and control, the gas turbine is equipped with many sensors. Due to long working hours under adverse conditions, the sensor may output abnormal signals, and then the monitoring signal will be delayed [15]. The typical five types of sensor faults are step fault, pulse fault, periodic fault, noise fault and drift fault [16-18]. In addition, the gas turbine control system is usually composed of measuring elements (sensitive elements), electronic controllers and actuators. The problems such as long sampling time, communication failure and long response time of actuators may occur during its work, which will result in delayed monitoring signal of the gas turbine.

The research of monitoring signal hysteresis mainly includes the use of fault-tolerant control and the establishment of fault diagnosis system. Since fault-tolerant control has the ability to reconstruct monitoring signals and can better maintain the stability of the control system, Hadroug [19-24] analyzed and discussed the application of fault-tolerant control. Fault tolerant control is mainly divided into two types: data-based fault-tolerant control and model-based fault-tolerant control. In terms of the current application of fault-tolerant control, it is difficult to realize data-based fault-tolerant control in engineering application. However, the existing model-based fault-tolerant control will degrade its fault-tolerant performance when the object does not match the observer model, and could not adapt to the characteristics of gas turbine with variable load. On the other hand, the robustness and reliability of the control system can be improved by establishing a fault diagnosis system [25]. The researches on fault diagnosis were also been paid more attentions, Rahmoune [26, 27] established a fault diagnosis system based on neural network and tested some faults. Ogaji [28] established a fault diagnosis system to solve the problem of sensor fault and reorganized the fault data into a fault-free form, this reconstructed data could be used to accurately perform sensor calculation. Considering that the performance degradation signs of the main components of the gas turbine are different at different operating points,

Mohammadi [29] proposed a fuzzy based FDI system with the help of load parameters as augmented input, which had robust performance against measurement uncertainty.

Monitoring signal hysteresis is a common problem in the operation of gas turbine. It can reduce the influence of monitoring signal hysteresis on the control system through fault tolerant control and fault diagnosis system. However, the influence way and principle of monitoring signal hysteresis on the control system are fuzzy. In this paper, an aero-derivative gas turbine for power generation is taken as the research object. Aiming at the problem of monitoring signal hysteresis, a monitoring signal hysteresis model is established, which is embedded into the digital simulation model to form a digital simulation model with the function of monitoring signal hysteresis. The control performance of this type of aero-derivative gas turbine is optimized. The above research results can provide an important reference for this type of aero-derivative gas turbine to reduce the impact of monitoring signal hysteresis.

2. ESTABLISHMENT OF DIGITAL SIMULATION SYSTEM

Using MATLAB/Simulink platform to establish digital simulation model is one of the important means of gas turbine research. The digital simulation model established in this paper is shown in Fig 1. The establishment process mainly includes four steps: firstly, based on the mechanism modeling method, the aero-derivative gas turbine model is established; Secondly, based on PID algorithm, the fuel quantity algorithm model is established; Thirdly, aiming at the problem of monitoring signal hysteresis, a monitoring signal hysteresis model is established; Finally, the three models are combined into a digital simulation model with the function of signal hysteresis monitoring.
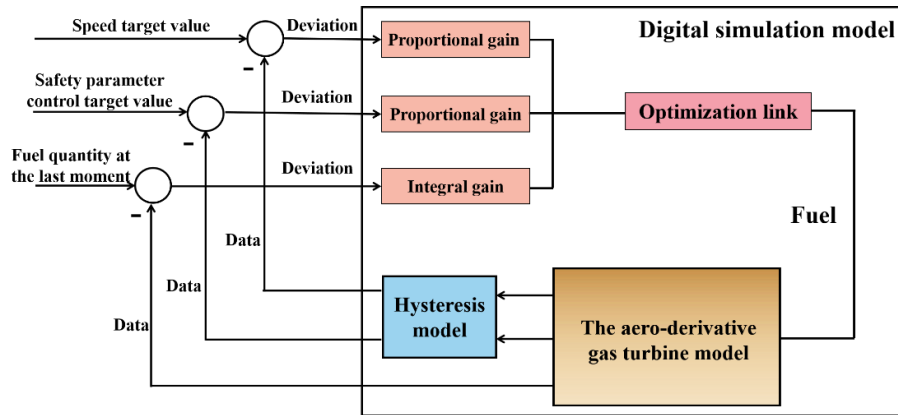
Fig. 1 Structure diagram of digital simulation model

2.1 The model of the aero-derivative gas turbine

The research object of this paper is an aero-derivative gas turbine for power generation. Its simplified structure is shown in Fig. 2, mainly including compressor, combustion chamber, turbine, power turbine, generator and other components. Gas turbine modeling methods are mainly divided into two categories: mechanism modeling and data modeling.

In the modeling process of aero-derivative gas turbine, due to the lack of measurement data such as high-temperature component measurement points and air side flow measurement points, the data modeling method is limited. However, the mechanism modeling method mainly depends on the physical mechanism of gas turbine components. Therefore, based on the mechanism modeling method, this paper establishes the model of aero-derivative gas turbine.
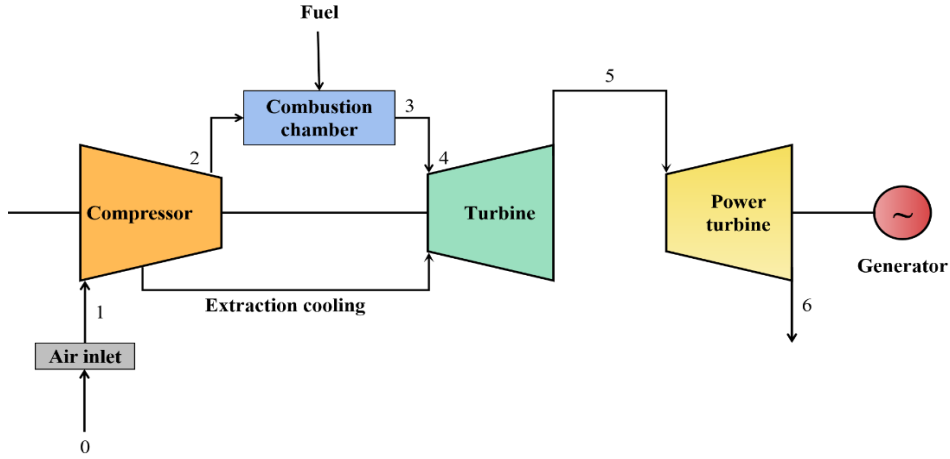
Fig. 2 Structural diagram of aero-derivative gas turbine

2.2 The model of fuel quantity algorithm

Fuel quantity is the most important control variable to change the operating state of gas turbine. By changing fuel quantity, the gas turbine can be controlled to complete acceleration or deceleration. The fuel quantity algorithm model mainly includes fuel quantity control algorithm and fuel quantity optimization link, which is used to receive the monitoring signal provided by the gas turbine model, calculate the fuel quantity, and feed back the fuel quantity to the gas turbine model.

2.2.1 Fuel quantity control algorithm

Due to the simple structure, good stability and reliable operation of the PID control algorithm, the PID control algorithm is used to construct the fuel control algorithm. The logic of the fuel algorithm consists of nine regulations, one being the primary one and the other eight being the limiting one, as shown in Table 1. It can be divided into speed control, safety limit control and fuel control according to its functions.

Based on the aforementioned fuel quantity algorithm logic, the fuel quantity PID control logic is designed. The control equation of each PID controller is shown in Eq. (1). Different from the traditional integral link, the variable integral gain coefficient is used in this paper, and the fuel increment in recent operation cycles is mainly used as the adjustment term to prevent excessive overshoot.

$$W_{fx} = K_p \Delta - \int_0^\tau K_I^{(\tau-t)} W_f(t-1) d_t \quad (t = 1,2,3,\ldots,\tau) \tag{1}$$

where W_{fx} is the fuel quantity difference, x is the different control variables substituted, K_P is the proportional gain coefficient, K_I is the integral gain coefficient, Δ is the deviation between the limit condition value or the target value of the control variable and the current state value, W_f is the fuel increment fed back after priority selection and τ is the number of control logic operations that have been run.

Table 1 Composition of fuel quantity algorithm logic

Number	Fuel quantity control sub circuit	Abbreviation	Type
1	Gas generator speed regulation	PID_GG	Main
2	Gas generator maximum speed limit regulation	PID_GGH	Limit
3	Gas generator acceleration limit adjustment	PID_NCA	Limit
4	Gas generator outlet temperature limit regulation	PID_T5	Limit
5	Compressor outlet pressure limit regulation	PID_P3	Limit
6	Compressor outlet temperature limit regulation	PID_T3	Limit
7	Maximum deceleration rate limit regulation	PID_NCD	Limit
8	Minimum fuel limit regulation	PID_WMIN	Limit
9	Maximum fuel limit regulation	PID_WMAX	Limit

2.2.2 Fuel quantity optimization logic

Since the MIN-MAX selector has multiple input items and only one output is executed, which can effectively limit the fuel quantity within the safe range, the fuel quantity optimization logic is designed by using the MIN-MAX selector. The designed fuel quantity optimization logic is shown in Fig. 3. It contains 9 input items and is selected in three steps, and finally outputs the fuel quantity that meets various restriction conditions.
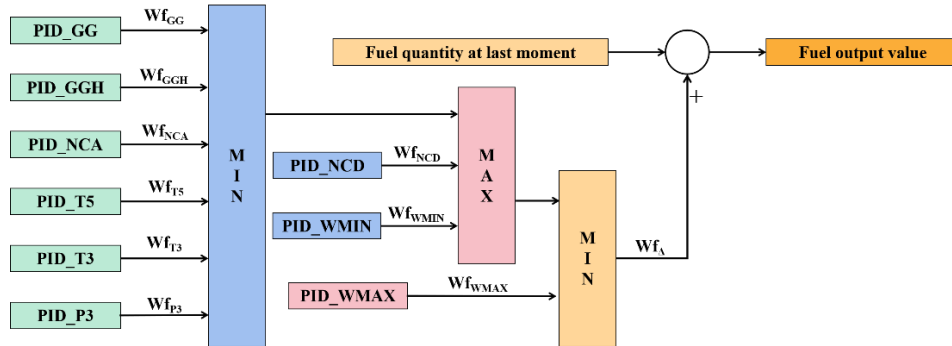
Fig. 3 Logical structure of fuel quantity optimization

The fuel priority selection logic is designed as a three-level priority with the following main functions:

a.   The first priority uses the minimum selector selection to ensure that the fuel increment obtained does not exceed the safety limit.

b.   Second priority uses maximum selector selection to ensure fuel increment is greater than PID_ WMIN to avoid lean oil extinguishing.

c.   The third priority uses the minimum selector to ensure that the final output fuel increment is less than the PID_ WMAX to prevent the gas turbine from rising too fast.

2.3 Hysteresis model of monitoring signal

In order to achieve the effect of monitoring signal transmitting real data periodically, a monitoring signal lag model is established based on the monitoring signal lag principle described in Eq. (2.a) and Eq. (2.b) Establishment of a hysteresis model by adding a zero-order retention module after the monitoring signal output module of the gas turbine model and providing a rate conversion module to ensure consistent sampling time. The sampling time of the zero-order hold module is hysteresis time, which can be set to 0.1s, 0.2s, etc. as needed.

$$nT \leq t \leq (n+1)T \quad n = 0,1,2,3 \dots \tag{2.a}$$

$$u(t) = u(nT) \qquad n = 0,1,2,3\dots \tag{2.b}$$

where T is the hysteresis time, t is the sampling time, $u(T)$ is the signal value at the current sampling time and $u(nT)$ is the signal value at the last sampling time.

3. EXPERIMENTAL SCHEME AND MODEL VERIFICATION

3.1 Experimental scheme

The monitoring signal hysteresis mainly comes from two aspects: sensor fault and control system fault. Although either cause has little impact on the speed control, the impact after the superposition of the two cannot be ignored. In order to explore the influence of single monitoring signal hysteresis on speed control, the experimental scheme is designed with pressure signal and speed signal as variables. In addition, the experimental scheme is designed by coupling speed signal and pressure signal and combining the analysis results of single signal hysteresis.

3.1.1 Experimental scheme of pressure signal

The proportional gain coefficient (K_P) in the fuel quantity algorithm is selected through the difference table, and the pressure signal is the input of the difference table. As the main influence factor of K_P, the pressure signal will lead to deviation in the selection of K_P once the hysteresis phenomenon occurs. Therefore, it is necessary to study the influence of the pressure signal hysteresis on the speed control. In order to obtain the influence law of pressure signal hysteresis on speed control, the selected pressure signal hysteresis time T_P as shown in Table 2, there are 10 experimental schemes.

Table 2 Pressure hysteresis time (T_P)

Plan	1	2	3	4	5	6	7	8	9	10
$T\_P(s)$	0.1	0.7	1.4	3.5	7	14	21	28	35	50

3.1.2 Experimental scheme of speed signal

The start-up stage of a gas turbine is usually judged by the gas generator speed. Once the speed signal is delayed, it will inevitably affect the judgment of the gas turbine start-up process. Therefore, it is necessary to study the effect of speed signal hysteresis on speed

control. In order to obtain the law of the influence of speed signal hysteresis on speed control, the selected speed hysteresis time T_S shown in Table 3, there are seven experimental schemes.

Table 3 Temperature hysteresis time (T_S)

Plan	1	2	3	4	5	6	7
$T\_S(s)$	0.1	0.2	0.3	0.4	0.5	1	3

3.1.3 Experimental scheme of coupling pressure signal and speed signal

As the gas turbine usually works in the environment of high temperature and high pressure, it is very easy to have problems such as sensor performance degradation and sensitivity deterioration. Therefore, it is necessary to consider the influence of various monitoring signal hysteresis, couple the pressure signal and speed signal, and design the coupling scheme according to the influence law of single signal hysteresis. The designed coupling scheme is shown in Table 4, including 9 coupling schemes.

Table 4 Hysteresis time coupling scheme of monitoring signal

Plan	1	2	3	4	5	6	7	8	9
$T\_P(s)$	0.1	0.1	0.1	14	14	14	35	35	35
$T\_S(s)$	0.1	0.5	1	0.1	0.5	1	0.1	0.5	1

3.2 Model validation

In order to verify the function of the hysteresis model of the monitoring signal, the hysteresis time of a single monitoring signal is calculated as a variable and compared with the parameters without hysteresis. The comparison results are shown in Fig. 4.
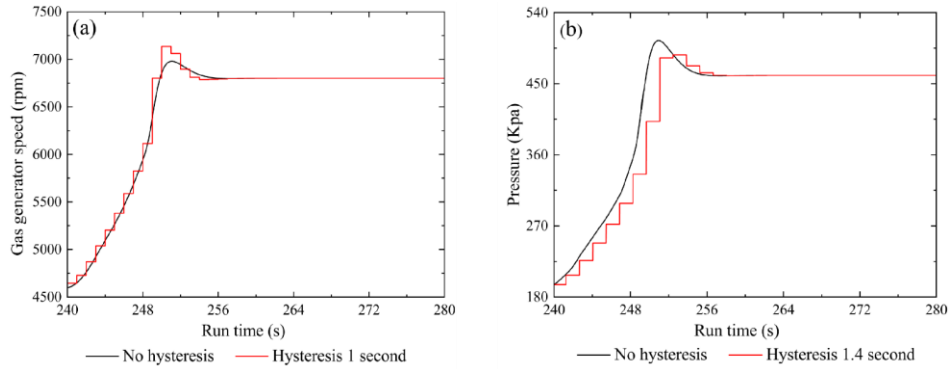
Fig. 4 Monitoring signal hysteresis curve: (a) Speed hysteresis, (b) Pressure hysteresis

From Fig. 4, it can be seen that the speed hysteresis curve is similar to the normal operation curve, and the hysteresis phenomenon is obvious. The pressure hysteresis will result in a smaller pressure output value, and the difference between the pressure hysteresis curve and the normal operating curve is a necessary phenomenon. Therefore, the

established monitoring signal hysteresis model has a good ability to reproduce the phenomenon of monitoring signal hysteresis.

4. EFFECT OF SINGLE MONITORING SIGNAL HYSTERESIS

4.1 Performance index

4.1.1 Adjustment time

Adjustment time is the shortest time that a controlled variable changes from a previous stable state to a new stable state when the control system is affected by external disturbances. In fact, the shortest time required for a control variable to enter a new steady-state value of ± 5% is called the adjustment time of the control system. The adjustment time is calculated as shown in Eq. (3):

$$T_S = T_2 - T_1 \tag{3}$$

where T_S is the adjustment time, T_2 is the time when the controlled variable reaches a new balance state, and T_1 is the time when the controlled variable begins to adjust.

4.1.2 Overshoot

The ratio of the maximum deviation of the adjustment parameter to the steady state value is called overshoot during the adjustment of the control system, and the maximum deviation refers to the deviation between the maximum value of the adjustment parameter and the steady state value. In this paper, for a clearer comparison and analysis, the maximum deviation of the adjustment parameters is defined as overshoot, and the overshoot is solved by Eq. (4):

$$\sigma = GG_{MAX} - GG_{SSV} \tag{4}$$

where σ is overshoot, GG_{MAX} is the maximum output value of the adjusted parameter, GG_{SSV} is the steady-state value of the adjusted parameter.

4.2 Effect of pressure signal hysteresis

In order to obtain the changing trend of gas generator speed when the pressure signal is hysteresis, the calculation is carried out according to the 10 pressure signal hysteresis schemes described in Table 2, and the calculation results are shown in Fig. 5.

It can be got from Fig. 5 that when the pressure signal hysteresis exists, the gas generator speed mainly presents four phenomena:

a.   The gas generator speed has obvious overshoot (the target speed is 6800rpm), and the overshoot gradually disappears with the increase of T_P.

b.   When the T_P exceeds 3.5 seconds, the speed of the gas generator remains at 4600 rpm, which is called the speed suspension phenomenon.

c.   When the T_P exceeds 35 seconds, the speed decreases. In the actual operation process, this phenomenon will trigger the downtime process.

d.   When the T_P exceeds 50 seconds, the speed of the gas generator cannot reach the speed demand value.
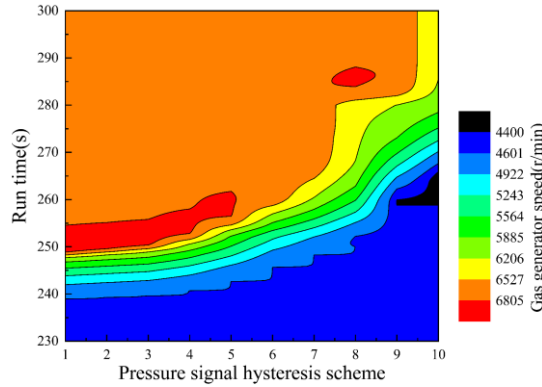
Fig. 5 Contour chart of gas generator speed when pressure signal is hysteresis

In order to further determine the influence of pressure signal hysteresis, the influence degree of pressure signal hysteresis on speed control is analyzed by taking performance parameters such as overshoot and adjustment time as evaluation criteria. The adjustment time and the solution of the overshoot follow Eq. (3) and Eq. (4) and the results are shown in Fig. 6.

As shown in Fig. 6, on the one hand, with the increase of T_P, the speed adjustment time gradually increases, and finally tends to 60 seconds, which fails to reach the target speed of 6800 rpm. On the other hand, with the increase of T_P, the speed overshoot decreases gradually, and eventually tends to -800rpm, which means that the speed fails to reach the expected target. Therefore, the pressure signal hysteresis will cause higher adjustment time for gas generator speed, and even make the speed cannot reach the target speed.
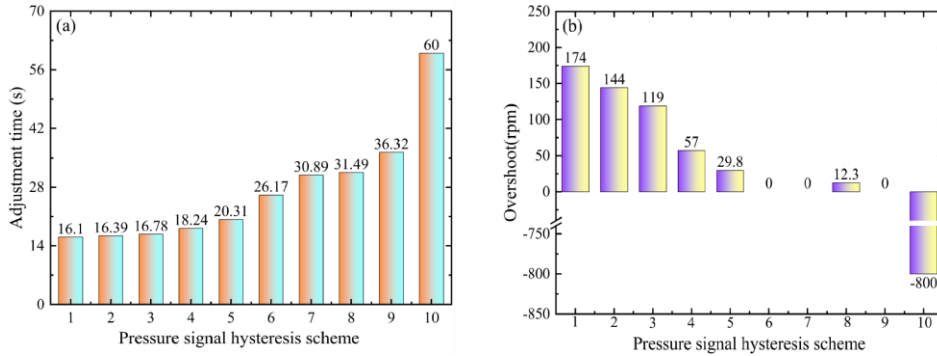
Fig. 6 Performance parameters for pressure signal hysteresis: (a) Adjustment time, (b) Overshoot

Since the fuel quantity is the main variable to control the speed, and the fuel quantity is selected by the nine types fuel quantity regulation output through the fuel quantity optimization logic, in order to further analyze the reasons for the above phenomena, the selected data are shown in Fig. 7 and Fig. 8.
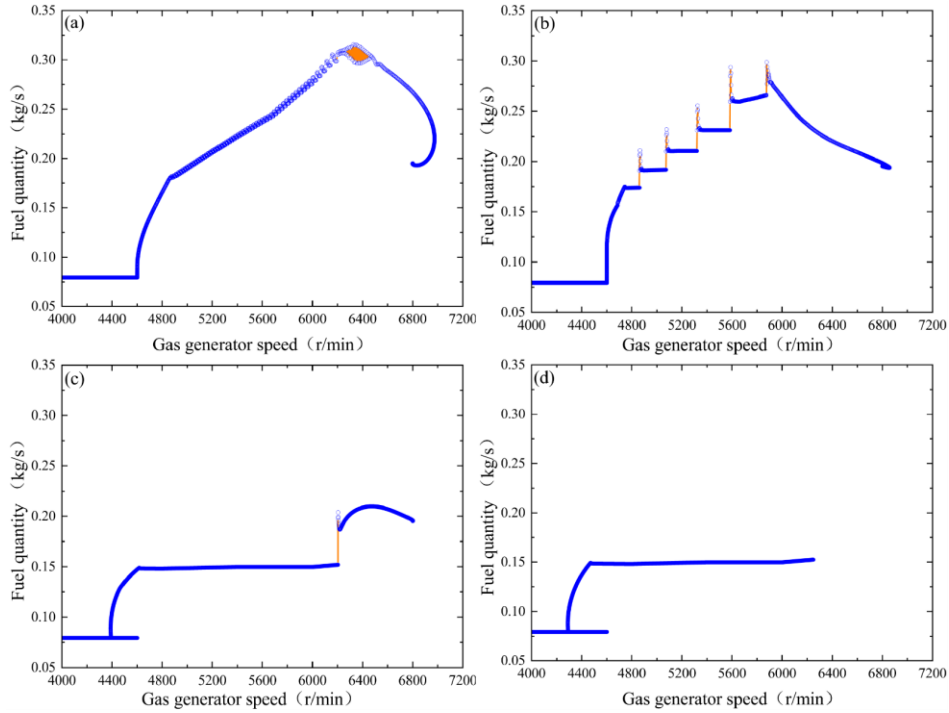
Fig. 7 Fuel quantity curve with pressure signal hysteresis: (a) *T_P*=0.1s, (b) *T_P*=3.5s, (c) *T_P*=35s, (d) *T_P*=50s

Since the fuel quantity is the main variable to control the speed, and the fuel quantity is selected by the nine types fuel quantity regulation output through the fuel quantity optimization logic, in order to further analyze the reasons for the above phenomena, the selected data are shown in Fig. 7 and Fig. 8.

As shown in Fig. 7, fuel quantity and *T_P* is inversely proportional, and there is a step supply phenomenon. The main manifestation is that when *T_P* is small, the fuel quantity curve fluctuates sharply. When *T_P* is large, the fuel quantity curve gradually flattens and presents a step supply phenomenon, which ultimately results in a slow increase in gas turbine speed.

As shown in Fig. 8, with the increase of *T_P*, PID_GG and PID_WMAX show different degrees of hysteresis phenomenon, and PID_P3 is always larger than PID_GG and PID_WMAX, which has no effect on the results of fuel optimization. Further analysis of PID_GG and PID_WMAX reveals that the main reasons for this phenomenon are:

a.   The proportional gain factor (KP_GG) of the PID_GG is determined by the outlet pressure of the compressor. The principle is that the pressure at the outlet of the compressor is used as the input of the two-dimensional difference table, KP_GG is selected, and PID_GG is calculated. Once the outlet pressure of the compressor is hysteresis, the selected value of KP_GG cannot meet the speed adjustment requirements, and the speed of the gas generator rises slowly.

b.   Compressor outlet pressure is directly involved in the calculation of PID_WMAX.

When the pressure at the outlet of the compressor is lagged, the calculated value of PID_WMAX is smaller, which results in a smaller result of fuel quantity optimal selection, insufficient fuel supply, and the gas generator speed is difficult to reach the target value.
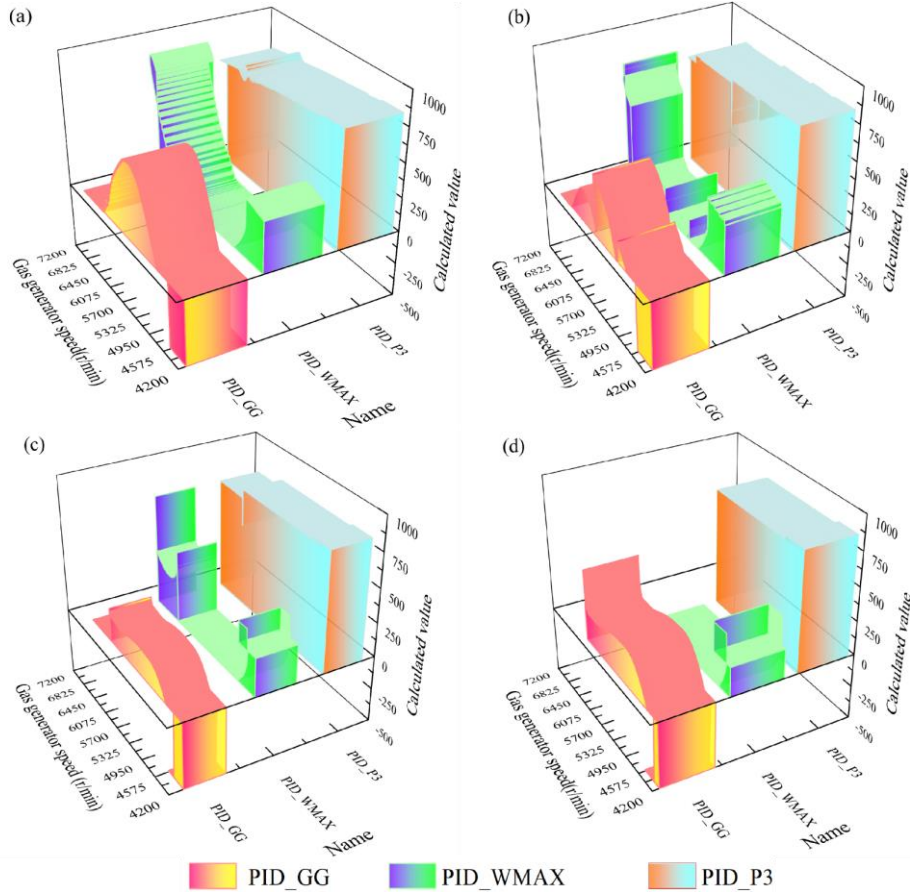
Fig. 8 Fuel quantity regulation output curve with pressure signal hysteresis: (a) T_P=0.1s, (b) T_P=3.5s, (c) T_P=35s, (d) T_P=50s

4.3 Effect of speed signal hysteresis

In order to obtain the changing trend of gas generator speed when the speed signal is hysteresis, the calculation is carried out according to the 7 speed signal hysteresis schemes described in Table 3. The calculation results are shown in Fig. 9.

In order to further determine the influence of speed signal hysteresis, the influence of speed signal hysteresis on speed control is analyzed by taking performance parameters such as overshoot and adjustment time as evaluation criteria. The corresponding adjustment time and overshoot, which are settled according to Eq. (3) and Eq. (4), are shown in Fig. 10.

It can be seen from Fig. 10 that when the speed signal is hysteresis, the gas generator speed mainly exhibits two phenomena:

a.   With the increase of T_S, the gas generator speed gradually tends to steep and the peak gradually increases.

b.   With the increase of T_S, the gas generator speed curve shows a stepped upward trend in varying degrees. When T_S is 3 seconds, the gas generator speed curve cannot reach a steady state, and fluctuates repeatedly in the range of 6000 rpm to 7800 rpm.
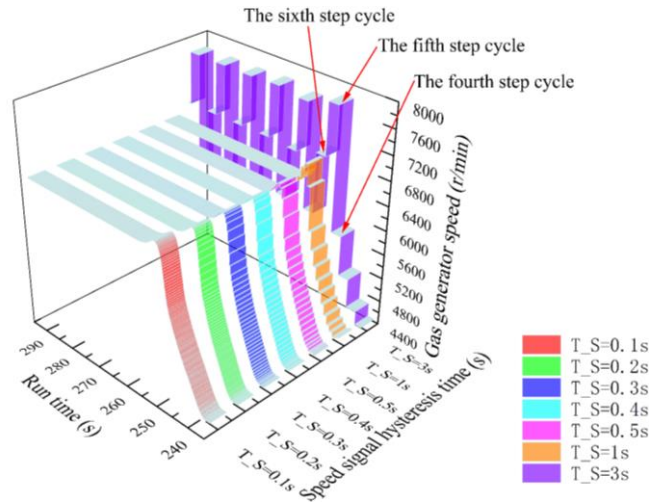
Fig. 9 Gas generator speed curve with speed signal hysteresis
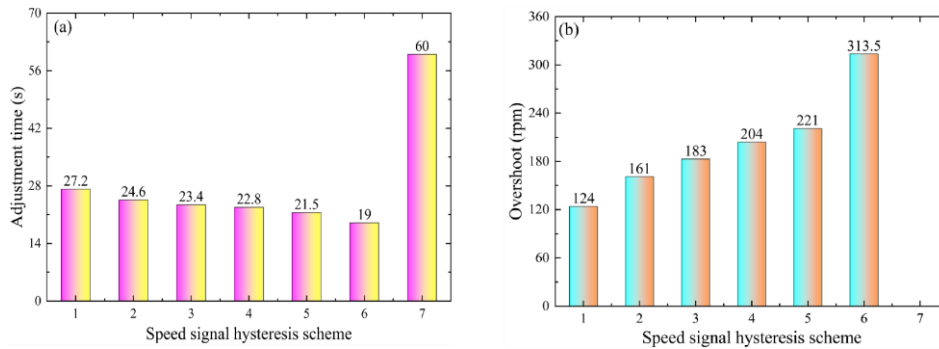
Fig. 10 Performance parameters for speed signal hysteresis: (a) Adjustment time, (b) Overshoot

On the one hand, the adjustment time is inversely proportional to T_S, on the other hand, with the increase of T_S, the overshoot increases gradually. When T_S is 3 seconds, the overshoot and adjustment time are difficult to calculate due to the sharp fluctuation of speed, so the adjustment time is the maximum of the expected adjustment time.

Using the same analysis method as pressure signal hysteresis, the influence mechanism of speed signal hysteresis is analyzed. The selected data are shown in Fig. 11 and Fig. 12. From Fig. 11, it can be seen that with the increase of T_S, the amount of fuel increases

gradually, the degree of chaos decreases, and the cycle regulation mode tends. From Figure 12, with the increase of T_S, the step phenomenon becomes obvious, the step number decreases, and the chaos degree of fuel optimization results decreases.

The main reason for the above phenomenon is that when there is a velocity signal hysteresis, the speed adjustment is equivalent to the multiple step adjustment mode. The number of steps is inversely proportional to T_S, the period of steps is positively proportional to T_S.

a.   When T_S is small, the number of steps is large and the step cycle is short. In order to meet the requirements of speed adjustment, fuel adjustment changes frequently, resulting in sharp fluctuations in fuel quantity.

b.   With the increase of T_S, the number of steps decreases and the period of steps increases. At this time, the speed adjustment is closer to the target, and the fluctuation of fuel quantity and fuel quantity regulation is reduced.

c.   When T_S is 3 seconds, the number of steps is the smallest and the step cycle is the longest. As shown in Figure 9, during the fourth step cycle, it is always considered that the speed does not reach the target value, the fuel quantity and fuel quantity adjustment continue to increase and exceed the demand value. During the fifth step cycle and sixth step cycle, the rotation speed starts to revert, and the fuel and fuel adjustments continue to decrease and fall below the demand value. Rotation speed adjustment shows cyclic regulation, which is manifested by repeated fluctuations of rotation speed in the range of 6000rpm to 7800rpm.
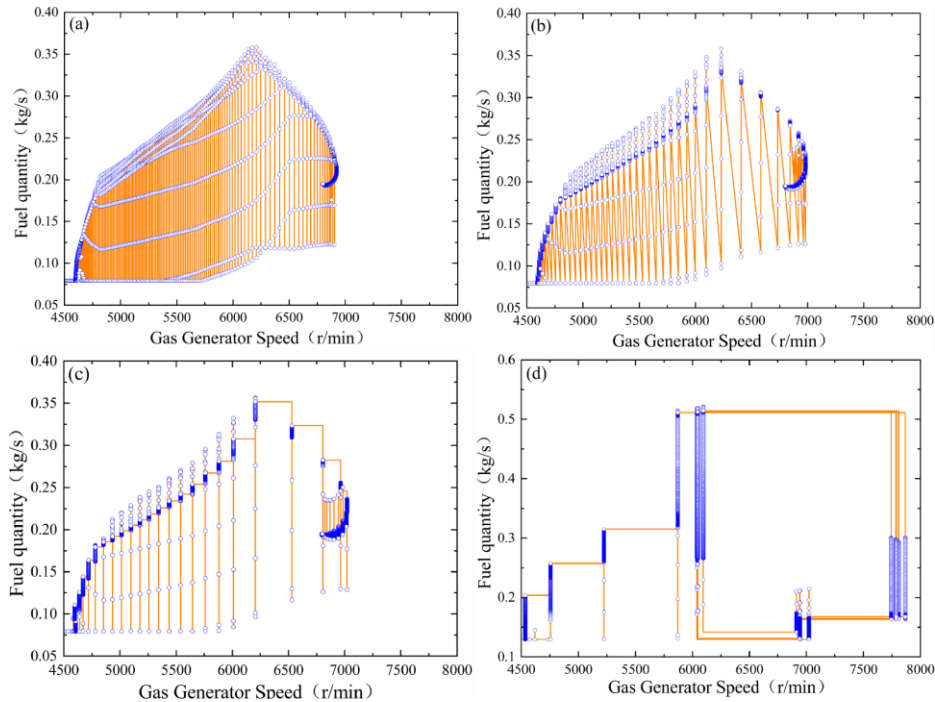
Fig. 11 Fuel quantity curve with speed signal hysteresis: (a) T_S=0.1s, (b) T_S=0.3s, (c) T_S=0.5s, (d) T_S=3s
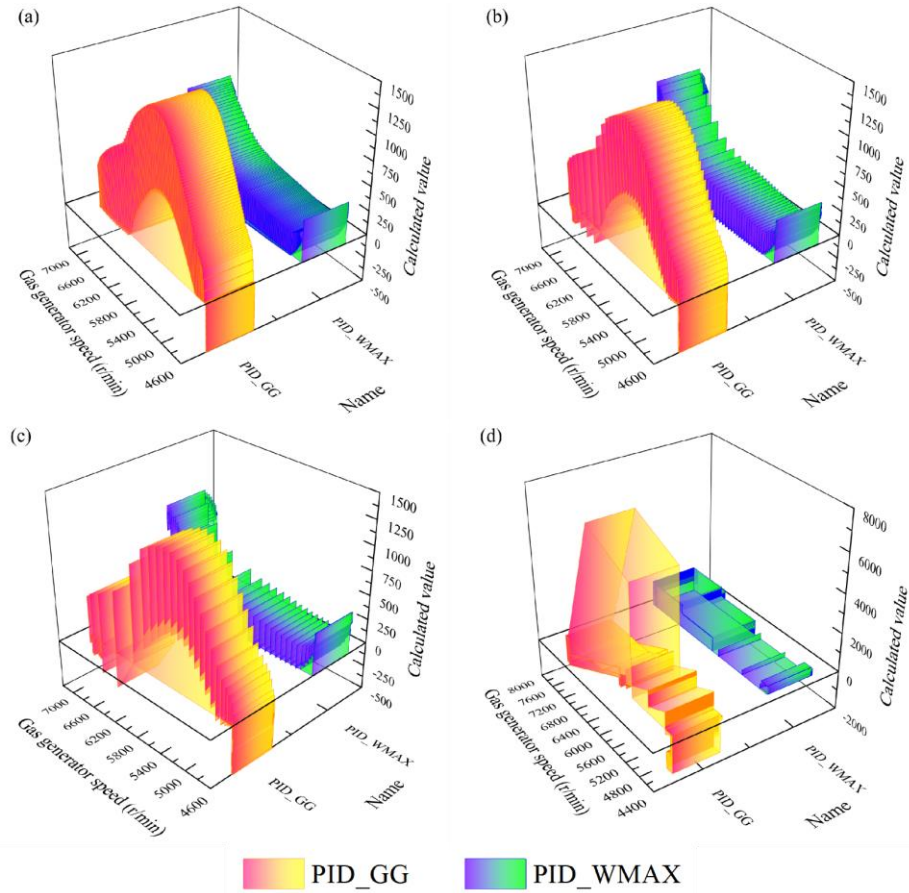
Fig. 12 Output curve of fuel quantity regulation in case of speed signal hysteresis: (a) *T_S*=0.1s, (b) *T_S*=0.3s, (c) *T_S*=0.5s, (d) *T_S*=3s

5. INFLUENCE OF HYSTERESIS COUPLING OF MONITORING SIGNAL

In order to obtain the speed control performance of multiple monitoring signals with hysteresis coupling, a coupling scheme is designed according to the influence rule of single monitoring signal hysteresis, which is used to calculate the gas generator speed as shown in Table 4. Deep analysis is made from the angle of control performance parameters, fuel quantity and fuel quantity adjustment. The calculation results of the gas generator speed are shown in Fig. 13. The main variation rules of the speed are as follows:

a.   When *T_P* is constant, the gas generator speed curve tends to steep with the increase of *T_S*, and the more obvious peaks occur when *T_P* is 0.1 seconds.

b.   When *T_S* is constant, the gas generator speed curve tends to be flat with the increase of *T_P*, and secondary regulation occurs when *T_S* is 35 seconds.
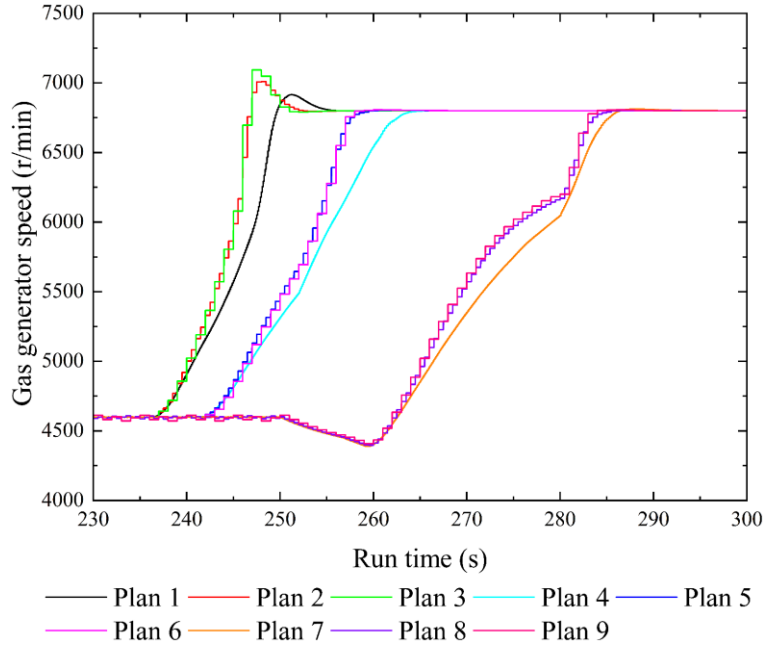
Fig. 13 Monitor the gas generator speed when the signal is hysteresis coupling
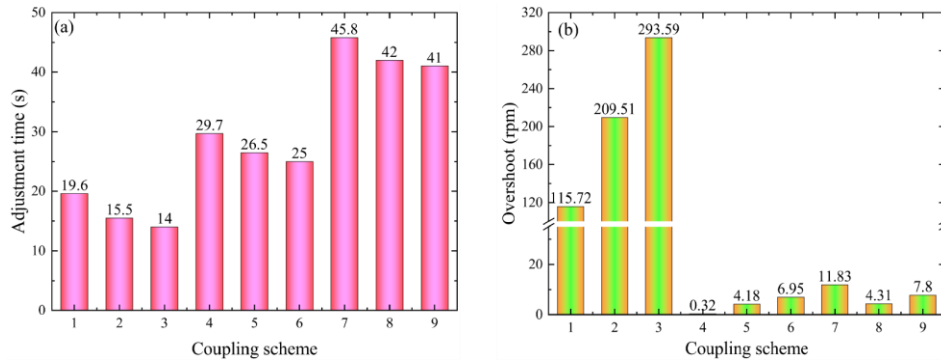
Fig. 14 Speed performance when monitoring signal hysteresis coupling: (a) Adjustment time, (b) Overshoot

The adjustment time and overshoot are calculated and analyzed by Eq. (3) and Eq. (4). The calculation results of adjustment time and overshoot are shown in Fig. 14. As shown in Fig. 14, on the one hand, the adjusting time is mainly affected by T_P, and the adjusting time is proportional to T_P, the adjusting time decreases slightly when T_S increases. On the other hand, pressure signal hysteresis has a great effect on overshoot, and the overshoot is inversely proportional to T_P, the overshoot increases slightly with T_S increases.
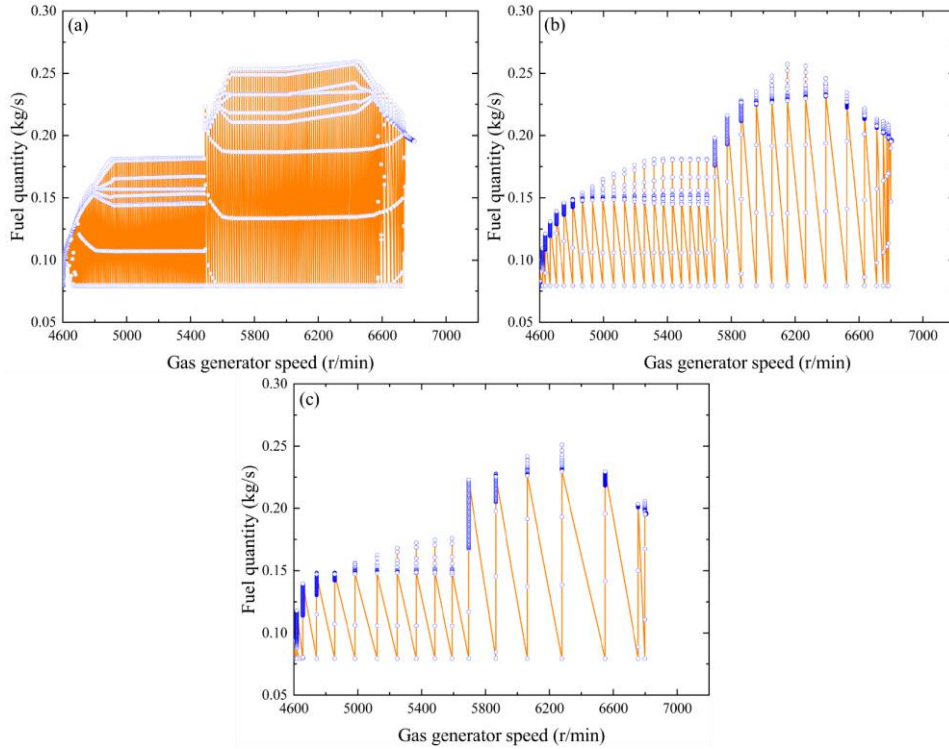
Fig. 15 Fuel quantity curve under hysteresis coupling of monitoring signal: (a) Plan 4, (b) Plan 5, (c) Plan 6

In order to further analyze the mechanism of the effect of the hysteresis coupling of the monitoring signal on the speed control, a discussion is made from the angle of fuel quantity and fuel quantity regulation, which is shown in Fig. 15 and Fig. 16. As shown in Fig. 15, the fuel quantity curves of the three coupling schemes have the same trend with only different oscillations. Both T_P and T_S in plan 4 are smaller, resulting in smaller proportional gain factor, more steps and shorter step cycle, and sharp fluctuation of fuel quantity curve. As T_P increases, the fluctuation of the fuel quantity curve decreases. Therefore, the influence on the speed adjustment is the overlap of pressure hysteresis and speed hysteresis after the monitoring signal hysteresis coupling.

The main reasons for the above changes are as follows: firstly, the coupling of pressure signal hysteresis and speed signal hysteresis will not only affect the selection of proportional gain coefficient and the calculation value of maximum fuel quantity in the output of fuel quantity regulation, but also change the speed regulation into a multi-step regulation mode. Secondly, the pressure signal is one of the main parameters in the fuel quantity algorithm. Compared with the speed signal, the pressure signal has a more direct influence on the fuel quantity control. Thirdly, the speed signal hysteresis only affects the speed adjustment mode, making the speed more tend to the multi-step adjustment mode, and the impact on the fuel quantity control is indirect.
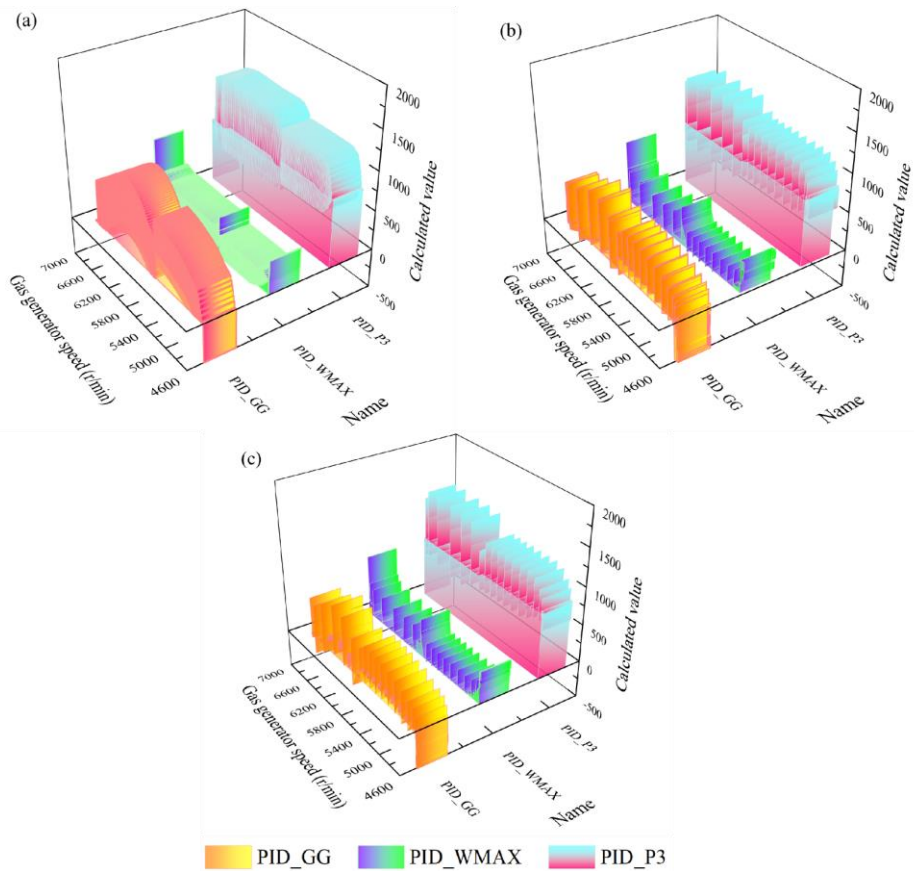
Fig. 16 Output curve of fuel quantity regulation under hysteresis coupling of monitoring signal: (a) plan 4, (b) Plan 5, (c) Plan 6

6. CONCLUSION

This paper takes an aero-derivative gas turbine for power generation as the research object and carries out two aspects of research. On one hand, the influence of pressure signal hysteresis and speed signal hysteresis on speed control is studied. On the other hand, the influence of monitoring signal hysteresis coupling on the speed control is also considered. The main conclusions are as follows:

1．Hysteresis of pressure signal will affect the selection of proportional gain coefficient and the calculation of maximum fuel quantity limit value, resulting in deviation of fuel quantity supply, speed suspension of gas turbine and even trip failure.

2．The speed signal hysteresis changes the speed control into a multi-step regulation mode, which results in frequent changes and confusion of fuel supply, serious overshoot of gas generator speed and even speed oscillation.

3．The effects of pressure signal hysteresis and speed signal hysteresis will be

combined when the coupling monitoring signal hysteresis is considered, and pressure signal hysteresis is the main influencing factor, resulting in very complex speed adjustment and a longer time for gas generator speed adjustment.

REFERENCES

1. Wang, G., Ge, N., Zhong, D., 2020, *Numerical investigation of the wake vortex-related flow mechanisms in transonic turbines*, International Journal of Aerospace Engineering, 2020, 8825542.
2. Scotti Del Greco, A., Jurek, T., Michelassi, V., Di Benedetto, D., 2021, *Design, Testing, and Performance Impact of Exhaust Diffusers in Aero-Derivative Gas Turbines for Mechanical Drive Applications*, Journal of Turbomachinery, 143(6), 061016.
3. Vyncke-Wilson, D., 2013, *Advantages of aero-derivative gas turbines: technical & operational considerations on equipment selection*, Proc. 21th Power-Gen Asia Conference, Bangkok, pp. 1-11.
4. Turan, O., Aydin, H., 2014, *Exergetic and exergo-economic analyses of an aero-derivative gas turbine engine*, Energy, 74, pp. 638-650.
5. Haglind, F., Elmegaard, B., 2009, *Methodologies for predicting the part-load performance of aero-derivative gas turbines*, Energy, 34(10), pp. 1484-1492.
6. Sylvestre, R.A., Dupuis, R.J., 1990, *The evolution of marine gas turbine controls*, Journal of Engineering for Gas Turbines and Power, 112(2), pp. 176-181.
7. Peltier, R., 2003, *Gas turbine combustors drive emissions toward nil*, Power, 147(2), pp. 23-34.
8. Tsai, A., Pezzini, P., Tucker, D., Bryden, K.M., 2019, *Multiple-Model adaptive control of a hybrid solid oxide fuel cell gas turbine power plant simulator*, Journal of Electrochemical Energy Conversion and Storage, 16(3), 031003
9. Qiu, C., Song M., 2009, *Remote control network system for brillouin scattering distributed optic fiber sensor based on embedded technology,* Chinese Journal of Sensors and Actuators, 22(5), pp. 684-687.
10. de Castro-Cros, M., Rosso, S., Bahilo, E., Velasco, M., Angulo, C., 2021, *Condition assessment of industrial gas turbine compressor using a drift soft sensor based in autoencoder*, Sensors, 21(8), 2708.
11. Yenchev, S.V., Mazur, T.A., Tovkach, S.S., 2018, *Fuzzy automatic control system synthesis of the propeller fan the aviation gas turbine engine*, Electronics & Control Systems, 4(58), pp. 56-63.
12. Yu, B., Cao, C., Shu, W., Hu, Z., 2017, *A new method for the design of optimal control in the transient state of a gas turbine engine*, IEEE Access, 5, pp. 23848-23857.
13. Ahmed, J.M., 2020, *Optimal tuning linear quadratic regulator for gas turbine by genetic algorithm using integral time absolute error*, International Journal of Electrical and Computer Engineering, 10(2), pp. 1367-1375.
14. Zhang, L., Li, S., Xue, Y., Zhou, H., Ren, Z.Y., Tsinghua U., 2022, *Neural network PID control for combustion instability*, Combustion theory and modelling, 26(2), pp. 383-398.
15. Sun, R., Shi, L., Yang, X., Wang, Y., Zhao, Q., 2020, *A coupling diagnosis method of sensors faults in gas turbine control system*, Energy, 205, 117999.
16. Chen, J., Wang, Y., Weng, S., 2011, *Application of wavelet singular entropy in periodic fault detection of sensors on gas turbines*, Noise and Vibration Control, 31(6), pp. 156-160.
17. Yu, B., Liu, D., Zhang T., 2011, *Fault diagnosis for micro-gas turbine engine sensors via wavelet entropy*, Sensors, 11(10), pp. 9928-9941.
18. Chen, J., Wang, Y., Weng, S. L., 2009, *Application of general regression neural network in fault detection of exhaust temperature sensors on gas turbines,* Proceedings of the Chinese Society of Electrical Engineering, 29(32), pp. 92-97.
19. Hadroug, N., Hafaifa, A., Batel, N., Kouzou, A., Chaibet, A., 2018, *Active fault tolerant control based on a neuro fuzzy inference system applied to a two shafts gas turbine*, Applied Artificial Intelligence, 32(6), pp. 515-540.
20. Ma, Z., Tong, S., Li, Y., 2016, *Fuzzy adaptive state-feedback fault-tolerant control for switched stochastic nonlinear systems with faults*, Neurocomputing, 186, pp. 35-43.
21. Shi, F., Patton, R., 2015, *An active fault tolerant control approach to an offshore wind turbine model*,

Renewable Energy, 75, pp. 788-798.

22. Wu, L. B., Yang, G. H., 2014, *Robust adaptive fault-tolerant control for a class of uncertain nonlinear systems with multiple time delays*, Journal of Process Control, 41, pp. 1-13.

23. Salahshoor, K., Kordestani, M., 2014, *Design of an active fault tolerant control system for a simulated industrial steam turbine*, Applied Mathematical Modelling, 38(5-6), pp. 1753–1774.

24. Lan, J., Patton, R. J., 2016, *A new strategy for integration of fault estimation within fault-tolerant control*, Automatica, 69, pp. 48-59.

25. Guasch, A., Quevedo, J., Milne, R., 2000, *Fault diagnosis for gas turbines based on the control system*, Engineering Applications of Artificial Intelligence, 13(4), pp. 477-484.

26. Yang, X., Bai, M., Liu, J., Liu, J., Yu, D., 2021, *Gas path fault diagnosis for gas turbine group based on deep transfer learning*, Measurement: Journal of the International Measurement Confederation, 181, 109631.

27. Salahshoor, K., Khoshro, M. S., Kordestani, M., 2011, *Fault detection and diagnosis of an industrial steam turbine using a distributed configuration of adaptive neuro-fuzzy inference systems*, Simulation Modelling Practice & Theory, 19(5), pp. 1280-1293.

28. Ogaji, S., Singh, R., Probert, S. D., 2002, *Multiple-sensor fault-diagnoses for a 2-shaft stationary gas-turbine,* Applied Energy, 71(4), pp. 321-339.

29. Mohammadi, E., Montazeri-Gh, M., 2015, *A fuzzy-based gas turbine fault detection and identification system for full and part-load performance deterioration*, Aerospace Science and Technology, 46, pp. 82-93.